Nanoscale Structures: Lability, Length Scales, and Fluctuations

Ellen D. Williams

Abstract

This article is an edited transcript based on the David Turnbull Lecture given by Ellen D. Williams of the University of Maryland on December 2, 2003, at the Materials Research Society Fall Meeting in Boston. Williams received the award for "groundbreaking research on the atomic-scale science of surfaces and for leadership, writing, teaching, and outreach that convey her deep understanding of and enthusiasm for materials research." This article focuses on the special properties of small structures that provide much of the exciting potential of nanotechnology. One aspect of small structures—their susceptibility to thermal fluctuations—may create or necessitate new ways of exploiting nanostructures. The advent of scanned probe imaging techniques created new opportunities for observing and understanding such structural fluctuations and the related evolution of nanostructure. Direct observations show that it is relatively easy for large numbers of atoms—the kinds of numbers that are present in nanoscale structures—to pick up and move about on the surface cooperatively with substantial impact on nano- to micron-scale structures. Such labile evolution of structure can be predicted quantitatively by using length-scale bridging techniques of statistical mechanics coupled with scanned probe observations of structural and temporal distributions. The same measurements also provide direct information about the stochastic paths of structural fluctuations that can be used outside of the traditional thermodynamic framework. Future work involves moving beyond the classical thermodynamic picture to assess the impact that the stochastic behavior has on the physical properties of individual nanostructures.

Keywords: *fluctuations, lability, mass transport, morphology, scanned probe microscopy, stability, nanocrystals, nanostructure.*

Introduction

It is a great honor for me to receive the David Turnbull Lectureship, and a special pleasure that Professor Turnbull himself was able to be present for this talk. In beginning this presentation, I would like to emphasize how old problems in materials science are revisited when new tools become available to address them or when new applications require a different perspective on previous understanding. In the work I will be discussing here, the old problem is surface mass transport, the new tool has been scanned probe microscopy, and the new application is nanoscale materials properties.

We can begin by asking what makes materials science special at the nanoscale? We do not expect nanoscale materials or systems to act like small-scale models of the macroscopic and effectively continuum world we live in. When we get down to the nanoscale, very different types of properties arise. One origin of novel properties for materials with size scales on the order of a nanometer is the large surface-to-volume ratio. When this is large, the special properties of surfaces such as quantum mechanical states that do not exist in the bulk (e.g., gap states that can create Fermi level pinning) can dominate the properties of the nanostructure. Another source of special properties at the nanoscale is entropy: when the number of particles in a structure is small, structural fluctuations can involve a large fraction of the volume, with the result that any individual nanostructure may deviate significantly from the average properties of a collection of nominally identical nanostructures.

Because these special nanoscale properties are directly related to the old problem of surface mass transport on solid materials, I will begin by placing the problem in historical context. Then I will go on to show some modern observations that demonstrate how easy it is to rearrange surface structure on the size scale of nanometers to microns. At these scales, we have the difficult problem that continuum approaches do not adequately address the atomistic nature of the structures, while atomistic approaches are too cumbersome for the relatively large number of atoms involved. A length-scale bridging approach, the continuum step model, allows us to address this problem; I will give some examples of how it is used experimentally to measure free energies and kinetic parameters and how it is applied to predict evolution of structure. We will end up looking beyond the classical perspective of deterministic mass transport and consider the implications of stochastic behavior at the nanoscale by applying new, non-thermodynamic methods for evaluating the predictability of measured structural fluctuations.

History

This problem of surface morphology and mass transport goes back a long time. It is humbling to look at some of the classical papers written in the 1950s; this early work set the cornerstones for everything we are able to do today in understanding structure at the nanoscale.

A key conceptual paper was "Some Theorems on the Free Energies of Crystal Surfaces" by Conyers Herring[1] on the stability of surface structures (see Figure 1a). He broke the conceptual barrier of a flat surface as a static entity by showing that if a flat surface does not represent a free energy surface on the equilibrium crystal shape, it will spontaneously break up into a hill-and-valley structure.[2–5] The mechanisms for that type of breaking up of the surface—large-scale diffusion causing the surface to change its morphology dramatically, as illustrated in Figure 1b—were then outlined about 10 years later by William Mullins in "Theory of Linear Facet Growth during Thermal Etching."[6] The key concepts presented by Mullins have been echoed in every subsequent advance

a

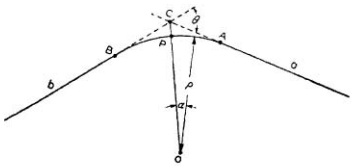

FIG. 4. Cross section of the surface of a crystal near where two flat faces a and b meet in a rounded edge.

b

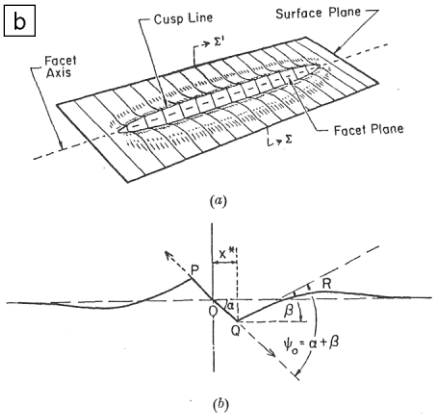

(a) A linear facet.
(b) Section Σ′ Σ of fig. 1 (a). Vertical exaggeration ~3×.

c

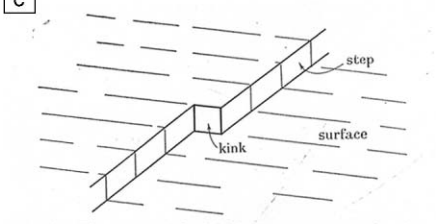

FIGURE 1. The presence of a kink in a step on a crystal surface.

Figure 1. Fundamental concepts in understanding the mobility of structures at surfaces were established in several classical papers written in the 1950s. (a) Conyers Herring's illustration that flat surfaces of arbitrary orientation are only stable when they correspond to a curved region of the equilibrium crystal shape.[1] (b) W.W. Mullins' illustration of the processes involved in evolution of a surface from flat to faceted.[6] (c) Burton, Cabrera, and Frank's illustration showing that surface steps serve as the fundamental point of action in surface mass transport.[7]

in understanding morphology evolution. Finally, the key underlying atomistic processes governing surface mass transport were delineated at least as early as 1951 by Burton, Cabrera, and Frank.[7] They identified the role of steps (shown in Figure 1c)—which I will later use as the ultimate nanoscale substructure—in governing the underlying mechanisms of surface mass transport in the evolution of surface structures.

To move from these papers to what we are able to do today required two important scientific breakthroughs. One was a theoretical understanding of entropy. At the time Burton, Cabrera, and Frank wrote their paper, nobody knew how to deal appropriately with the role of entropy in fluctuating steps (the analogous problem also arose in polymer physics). Mullins actually dealt with this problem in the mid-1960s,[8] but the general significance of his solution was not recognized until the 1980s.[9,10]

The second breakthrough that had to occur was in our ability to image the surfaces of small structures with atomic resolution. Until the early 1980s, aside from field ion microscopy,[11] we were not able to look at the distributions of structures in real space. Our measurements were of average properties of systems of structures. Information about structural distributions and fluctuations of individual nanostructures had to be deduced (generally with a high degree of non-uniqueness) from an interpretation of average measurements.

Beginning in the early 1980s, the development of scanning tunneling microscopy (STM),[12] as well as other innovative microscopies such as low-energy electron microscopy,[13,14] reflection electron microscopy,[15,16] and great improvements in environmental scanning and transmission electron microscopies (SEM and TEM), changed the way we could make experimental observations. With these techniques, we can look at systems and measure not just the average properties, but also the full distribution of properties about the average. We now can essentially do experimental statistical mechanics, where we map out the distribution of structures. From those, we can directly calculate partition functions that in turn yield all of the thermodynamic properties of the system.

Surface Lability

A natural consequence of a structure being a solid is that its shape is resistant to change. However, this intuition is misleading when one considers surface morphology. There, micron-scale rearrangements can occur at moderate temperatures via the relatively easy diffusion of atoms across the surface. We begin by considering one example of surface lability, the rearrangement of small Pb crystallites, a classical system for studies of equilibrium crystal shape.[17–20] Figure 2a is an STM image of the top of a ~1-μm-diameter crystallite supported on a ruthenium surface.[21] It was melted at ~300°C and slowly cooled, forming a flat facet on the top of the crystallite. Around the edges of the facet are concentric circular line boundaries; these are steps between the interatomic layers that terminate at the edge of the equilibrium crystal shape. As one moves down the edge of the crystal, the descent is not smooth. Instead, the descent occurs by a sequence of discrete steps, and the separation between adjacent steps (and thus the area of the flat regions between them) gets smaller as one moves downward, as shown in the histogram in Figure 2b. This illustrates an important concept: the sides of crystalline nanostructures of arbitrary shape can be described in terms of a "staircase" of steps that can serve as a source (or sink) of diffusing atoms.[22]

Surface lability is illustrated in the mass transport needed to form the flat-topped structure of Figure 2a from the original rounded structure at high temperature. The mechanism by which this change in shape occurs is illustrated in Figure 2c. This shows a time-lapse sequence of STM images following rapid cooling of a crystallite from high temperature. The gray-scale top view shows the top facet and the second layer. The top layer is shrinking; on the time scale of 30 min, it disappears entirely, and the second layer becomes the top layer. The process then repeats itself, with the new layer shrinking and so on for many tens of layers until the overall structure reaches a metastable or equilibrium state.

There are several things to note here. First, given that the top facet is ~350 nm in diameter, a quick calculation shows that each of these disappearing layers contains more than 500,000 atoms. So here we have about 500,000 atoms, picking up and moving someplace else in an apparently deterministic process, on a time scale of tens of minutes. Second, we can wonder about the strength of the driving force that causes this motion—and we'll answer that question later, after we've seen how to quantify chemical potentials. Third, the physical process going on here is easy to visualize—atoms are detaching from the step that bounds the top layer, then diffusing outward across the terrace, and reattaching at the edge of the crystallite. The process can be quantified, as illustrated in Figure 2d, which shows the diameter of the top two layers and the step–step separations around the edge of the crystallite through three cycles of layer removal. Finally, a small noise level is visible in the diameter of the top layers, and a much larger relative noise level shows up in the step–step separations. This is not instrumental noise. However, it is physical noise in the sense that it is a direct result of the thermal fluctuations of the nanostructure itself.

In the example of the Pb crystallite, the structure is relaxing into a new equilibrium state after an abrupt change in temperature has changed the free energy balance. A driving force for structural rearrange-

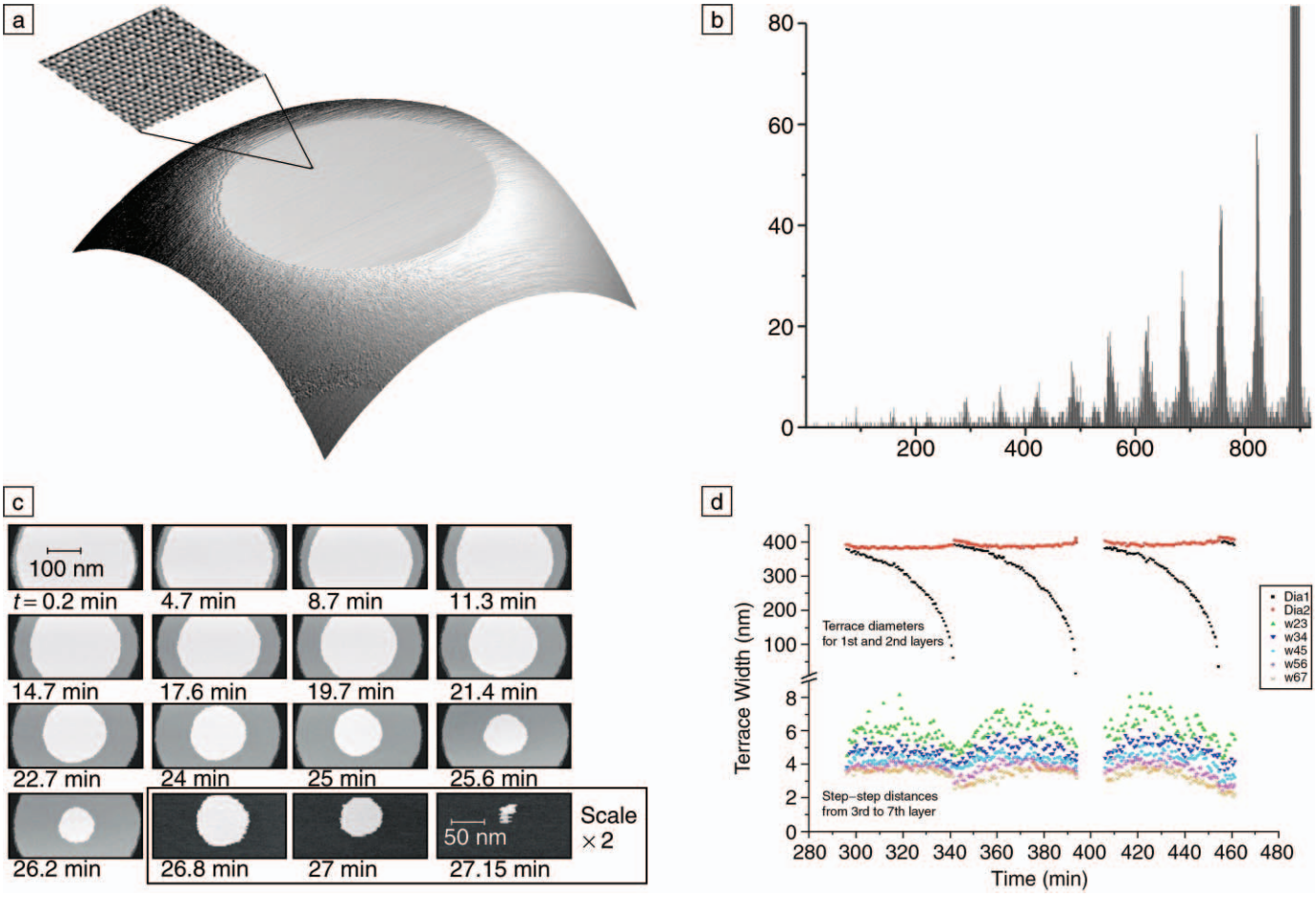

Figure 2. Surface mass transport results in the motion of steps (the boundaries of crystalline atomic layers) and large-scale changes in morphology, as illustrated for a near-equilibrium, micron-scale Pb crystallite measured with scanning tunneling microscopy. (a) Crystal shape after slow cooling from the melt and extended annealing at 110°C. The top facet shows atomic structure with (111) orientation. (b) Histogram showing the relative areas of the terraces between steps down the edge of the crystallite. The area of the top facet extends beyond the scale shown by about 40×. As one moves down the edge of the crystal (from right to left in the histogram), the distance between steps, and thus the relative area of the flat region between them, decreases. (c) Gray-scale top-view images of the evolution of the crystal through a change in height by one atomic layer at 80°C. (d) The diameters (Dia1, Dia2) of the top two layers as a function of time (black and red curves) and the distances between steps (w) along the crystallite edge. Images and analysis by K. Thümer, University of Maryland NSF-MRSEC.

ment can be imposed in other ways as well; for instance, the imposition of nonequilibrium concentration gradients by growth or sublimation,[23] changes in the free energy balance by chemical reaction,[24] or the extremely weak driving force of electromigration.[25–28] In all of these cases, the continuum step model provides a powerful tool for quantifying the lability that characterizes nanoscale structures.

Continuum Step Model

We want to be able to describe the structural rearrangements that occur at the nanoscale. This means describing structures that contain somewhere between tens of thousands to millions of atoms. We cannot do this properly using continuum dynamics because any sharp edges on a structure create discontinuities, and we don't have any way to independently determine the parameterization of a continuum dynamics approach. On the other hand, if we want to go to the full atomic scale, we have too many atoms, and potential energy surfaces that are too complex and diverse, to be able to address the problem. So we have to choose the right length-scale bridging approach.

As originally described by Burton, Cabrera, and Frank,[7] steps provide the length-scale bridging link between the atomistic and microscale properties of surface structure. The advances in statistical mechanics in understanding step properties[29] make it possible to quantify this link, which can be done using the continuum step model.[22,30–33] Here, I will show how we can use direct measurements to understand both the free energies governing step behavior and the kinetics of mass transport involving surface diffusion. Much more information can be found in recent reviews.[34,35]

The issues in describing steps are illustrated in Figure 3. At 0 K, perfectly ordered crystalline surfaces include perfectly ordered steps and kinks[36] (Figure 3a). Monte Carlo simulations allow the effects of temperature to be visualized and quantified (Figure 3b). Excitations of atoms from the terrace are energetically costly, but excitation at the step edge by kink formation occurs at moderate temperatures. The result is thermal wandering of the step. As one follows the path of the step—its perpendicular displacement x as a function of position y along the step—the wandering is similar to a random walk in which the walker can move zero or one units to the

right or left on each step forward in y. The specific prediction for the mean-square displacement for the step wandering is:

$$\langle (x(y) - x(0))^2 \rangle = \frac{kT}{\tilde{\beta}} y, \qquad (1)$$

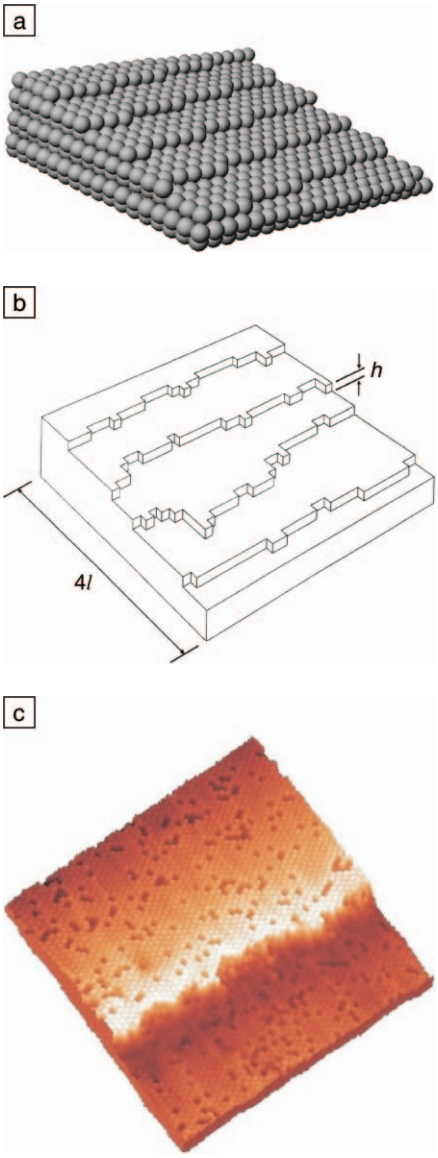

Figure 3. Three views of a step. (a) Perfectly ordered (T = 0 K) crystal structure with regular steps and regular kink density at the edge of the step.[36] (b) Monte Carlo simulation[37] of a stepped surface with average step–step spacing l in a square lattice model with only near-neighbor interactions. The energy scale is set by the kink formation energy ε. (c) Room-temperature scanning tunneling microscopy image of $(\sqrt{3} \times \sqrt{3})$R30° ordered Al overlayer on Si(111). Image size, 30 nm × 30 nm; step height, 0.31 nm.[39]

where $\tilde{\beta}$ is a thermodynamic quantity known as the step stiffness, k is the Boltzmann constant, and T is temperature. For the square lattice model of Figure 3b, the stiffness is a known function of the kink energy and temperature,[37] and more complex geometries can be solved as well.[38]

Such step wandering is immediately observable in the atomic-resolution image of real surfaces, as in the STM image shown in Figure 3c. This is an Al/Si(111) structure.[39] It is a well-ordered structure with some defects due to Al/Si exchange on the terraces. The step wandering takes place in units of the overlayer unit cell. This wandering can be compared directly to the Monte Carlo simulation of Figure 3b, keeping in mind that there is substantial atomic complexity (6 Si atoms and 1 Al atom) in each physical unit cell. However, in analyzing the step wandering using Equation 1, we do not have to worry about the underlying atomic structure, we just have to keep track of the shape of the step edge, $x(y)$. In fact, for this system, despite the atomic complexity, we find that Equation 1 is obeyed well over a broad temperature range (770–1020 K). This is not surprising—the random walk behavior is quite general. It is surprising, however, that the temperature dependence of the measured stiffness follows the predictions of the simple near-neighbor lattice model, yielding an *effective* kink energy of 0.2 eV.[39] Being able to predict the relationship between the thermodynamic behavior of the thermal step wandering and the underlying atomic interactions is a fundamental challenge that has only been addressed for simple systems.[40,41]

The step wandering also couples into another thermodynamic term—the step interaction free energy. The presence of neighboring steps constrains step wandering. This limits the step entropy, and so the free energy of confined steps is higher than that of free steps. Thus, there is an effective repulsion between steps that is strengthened by stress-mediated interactions.[42,43] Both the entropic and stress-mediated interactions fall off as the inverse square of the step separation. Measurement of the distribution of spacings between steps yields the strength of the step–step repulsion.[44,45] Given both the step stiffness and the step–step interactions, one can evaluate the chemical potential associated with any given step configuration. This concept is illustrated in Figure 4. An unconstrained step, which exists in equilibrium with a concentration c_0 of freely diffusing atoms, is defined as the zero of chemical potential. As a forced curvature is added to the step, or as steps are brought into proximity with neighboring steps, the chemical potential increases:

$$\mu_i = \Omega \left[\frac{\tilde{\beta}}{R} + \frac{gh^3}{2R} \left(\frac{1}{l_i^2} + \frac{1}{l_{i+1}^2} \right) - 2gh^3 \left(\frac{1}{l_i^3} - \frac{1}{l_{i+1}^3} \right) \right], \qquad (2)$$

where $\tilde{\beta}$ is the step stiffness, as in Equation 1; g is a coefficient determined by the strength of step–step repulsions;[44,45] Ω is the atomic area; R is the radius of curvature of the step; l_i and l_{i+1} are the distances to the steps on either side of the step of interest; and h is the step height.[46–48] The first term in Equation 2 is the traditional Gibbs–Thompson chemical potential for a curved interface, and the second[48] and third

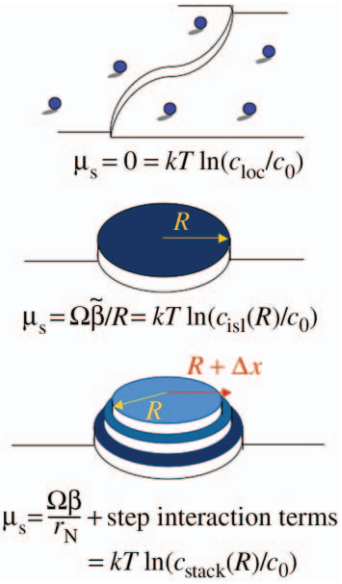

Figure 4. Nanoscale structures can be described as stacks of atomic layers bounded by edges of specific shape and slope. The local chemical potential at any point on the edge of a nanostructure is then defined by the geometry of the steps on the edge—most specifically, the radius of curvature and the distance to neighboring steps. The chemical potential of a step is related to an equilibrium concentration of freely diffusing atoms on the terraces above and below the step, with which there is balanced mass exchange at the step edge. For an isolated straight step (top illustration), the local concentration c_{loc} is identical to the equilibrium concentration c_0 of the flat surface. For a structure bounded by a curved step (center), the local concentration c_{isl} is larger than c_0, and the addition of a neighboring stack of steps (bottom) causes the local concentration c_{stack} to be larger yet.

terms are due to step–step interactions. The first and second terms disappear for an array of straight steps (e.g., R is infinite), leaving only step interactions to govern mass transport.

Overall, we can describe any given nanoscale geometry in terms of boundaries formed by steps and predict the chemical potential locally, as illustrated in Figure 4. Arbitrarily shaped structures will have different chemical potentials at different points on the structure, yielding the chemical potential gradients that will drive mass transport.

The second point to consider—and this will give us the information we need to predict the kinetics of mass transport—is that equilibrium is dynamic. In the image in Figure 3c, taken at room temperature, everything is frozen for this system: the temperature is too low to overcome diffusion barriers. The picture represents a snapshot of some configuration of thermal equilibrium formed at a higher temperature. When a system is actually in thermal equilibrium, there is always an exchange of atoms. So, if we heat a stepped surface to a temperature at which the atoms have enough mobility to achieve dynamic equilibrium, we start to see something new happen. That is, as we take images of the steps, the picture looks different every time. The reason for this is that the steps are moving (by atomic exchange). We see this experimentally in STM in the form of discontinuous displacements of the step edge as the image scan passes near the same point.[49,50] This is illustrated in Figure 5 for the same Al/Si(111) surface shown in Figure 3c, measured now with the sample held at 700°C.[39] Because we want to measure the position of the steps as a function of time, we measure repeatedly across one line perpendicular to the steps, rather than taking a full two-dimensional image. This is a real-time trace from which we can extract the position of the steps versus time $x(t)$.

The underlying physical basis for all this step motion is that atoms are moving around the step edge. They can move by hopping on and off the step edge, or they can move by atomic hopping parallel to the step edge. The motion of atoms causes the displacements of the edge of the step, as shown in Figure 5. As the steps fluctuate, the step stiffness exerts a restoring force to bring the step position back to the average. So, the overall rate of motion that we observe depends on both the time scale for atomic motion and the stiffness of the step. We can extract this information from the time correlation function $G(t)$ of the step fluctuations, which has a simple form, in simple cases (which are what have almost always been observed experimentally):[39]

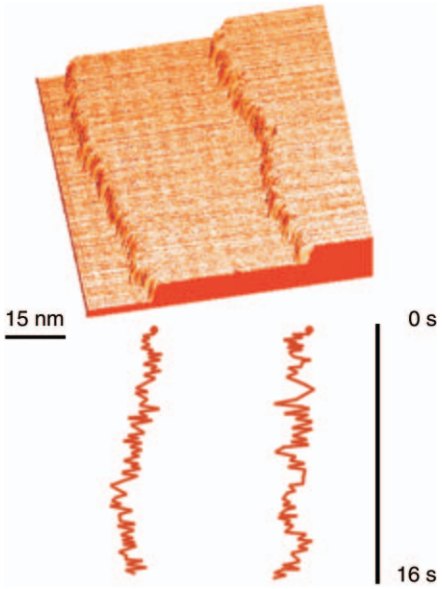

Figure 5. Repeated scanning tunneling microscopy scans across a 75 nm line perpendicular to two steps on Al/Si(111) at 700°C. The horizontal direction represents the position along the surface x, *the vertical distance represents time* t *as defined by the time interval between scans, which in this case is 41 ms. Extracting the step position from the scan yields* x(t), *as shown in the lower part of the figure.*[5]

$$G(t) = \langle (x(t) - x(0))^2 \rangle = \left(\frac{2\Gamma(1 - 1/n)}{\pi} \right) \left(\frac{kT}{\tilde{\beta}} \right)^{\frac{n-1}{n}} \left(a^{n+1} \frac{t}{\tau_n} \right)^{\frac{1}{n}}, \quad (3)$$

where x is the displacement of the step perpendicular to the average step edge orientation; t is time; a is the lattice constant; Γ is the gamma function; $\tilde{\beta}$ is the step stiffness; $n = 2$ or 4, depending on whether atoms attaching at the step edge or atoms diffusing parallel to the step edge dominate the motion; and τ_n is the time constant governing the relevant atomic motion. (For the complexities that can arise in a full treatment with competing mechanisms of atomic motion, see References 31 and 32.)

The analysis of step wandering data for Al/Si(111) using the time correlation function is shown in Figure 6. The shapes of the measured curves show that $n = 2$ (e.g., atomic attachment dominates mass transfer). The prefactors of fits of each of the individual data sets to Equation 3 yields the time constants, which vary with temperature from about 260 ms at 770 K down to 0.3 ms at 1020 K.[51] This means that at the lowest temperature, there are about four atomic exchanges per step edge site per second, while at the highest temperature, there are over 3000 exchange events per second. The temperature dependence is (as also was the case for the step stiffness) surprisingly simple—it follows an Arrhenius form with an *apparent* activation energy of 1.9 eV. Understanding what such an apparent activation energy means in terms of the underlying physical mechanism—in this case, for a unit cell of seven atoms—is a fundamental challenge. However, from the point of application, we can use the time constants measured in this way to predict nanoscale mass transport, even though we do not fully understand their physical meaning.

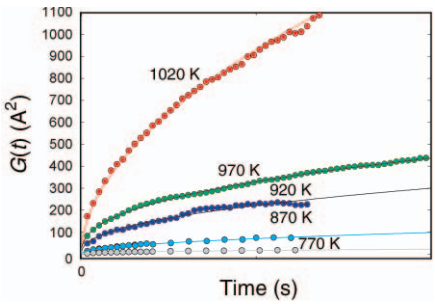

Figure 6. The time correlation function for Al/Si(111) determined from repeated scanning tunneling microscopy scan measurements, such as the one in Figure 5. The data are fitted to a power law in time with an exponent of 0.47 ± 0.04, indicating that the rate-limiting process for step motion is the exchange of atoms between the step and the terrace. The prefactor of the fit yields the time constant of the atomic exchange, which decreases from 260 ms at 770 K to 0.3 ms at 1020 K. Typically, 5–20 x(t) *(position–time) data sets are needed to have sufficiently good statistics to evaluate the correlation function.*

Nanoscale Mass Transport

Now we would like to take these ideas—the free energies that we obtain by measuring the spatial distribution functions and the time constants that we can get by measuring the temporal fluctuations of the steps—and use them to predict mass transport. I will take two examples: some Si nanostructures fabricated by the group of Professor Ichimiya of Nagoya University, and the Pb crystallite discussed earlier. For each initial structure, we will define the structure in terms of the position of the steps and assign a chemical potential (see Figure 4) using measured values for step

stiffness and step interactions. Then, we will calculate how fast each step moves, based on its chemical potential compared with those of its neighbors. We are going to get these rates right—without arbitrary fitting parameters—because the rate will be directly related to the time constant that we determined from our equilibrium fluctuation measurements. For any arbitrary structure that we start with, we can solve the equations of motions (numerically, if need be) for the whole array of steps, and we can predict the mass transport over large-scale distances.[27,46]

The case of the Si nanostructure is illustrated in Figure 7. The nanostructures are fabricated using the STM tip and are metastable; as soon as the temperature is high enough to enable atomic diffusion, the structures decay.[52] The rate of the decay has been measured by time-lapse STM images of the entire structure, which show that the structure evolves in a layer-by-layer process: the top layer breaks loose from the edges of the structure, shrinks, and disappears, followed by the second layer, until the entire structure disappears. Careful data analysis also yields detailed geometrical information on the height of the structure and the area of each layer as a function of time. The use of the continuum step model to describe this process, taking the very simplest model of a stack of circular layers, is illustrated in Figure 7b. For attachment-limited kinetics, each step in the cone will move with a radial velocity:

$$\frac{dr_n}{dt} = \frac{a}{2\tau_2 kT}(2\mu_n - \mu_{n+1} - \mu_{n-1}), \qquad (4)$$

where the step chemical potentials are defined as per Equation 2.

By making the assumption that the slope of the cone remains constant, the coupled equations of motion of Equation 4 yield a simple analytical solution:[47,53]

$$z_0 - z(t) = \left[\frac{4h^2a^3\tilde{\beta}t}{m^2kT\tau_2}\right], \qquad (5)$$

where z is the height of the cone; h and a are the step height and lattice constant, respectively; and m is the slope of the cone. Because the radius of curvature is small, the step repulsion term is insignificant in comparison with the effect of the stiffness. The predicted 1/4 power-law time dependence of the decay is confirmed by the experimental measurements of height versus time.[54] Somewhat surprisingly, given the simple model (the model of circular layers neglects the clear evidence of edge facets on the cone in Figure 7a), the prefactor of the fit to Equation 5 yields a value within a factor of two of the value predicted using an independent measurement of the ratio of $\tilde{\beta}/\tau_2$.[53] The evidence, therefore, is that the continuum step model works well down to length scales of nanometers, where one would have expected that the discrete nature of kinks and facets on the step edge would become important. Another interesting result is the magnitude of the driving force for the decay. Using Equation 2 for the step chemical potential, we find that the driving force is only about 0.4 kT. Using the perspective of atoms fluctuating on and off the step edge, this is equivalent to only 1 in 15 fluctuation events resulting in an atom permanently leaving the step edge. So, although the overall decay of the structure appears quite deterministic, there is a significant underlying stochasticity to the process.

A second example, the relaxation of the Pb crystallite (illustrated in Figure 2), is similarly amenable to quantitative analysis using the continuum step model. In this case, the starting configuration for the decay is a high-temperature structure that has been quenched to a lower temperature at which the thermodynamic parameters are different. This upsets the chemical potential balance and mass transfer results, yielding layer-by-layer peeling, which is easily visualized in terms of the radii of the top two layers as a function of time (Figure 8a).

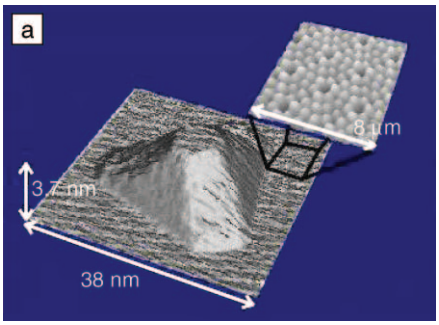

Figure 7. Nanostructure evolution can occur if the fabrication process creates a metastable structure subject to decay at temperatures at which diffusion is activated. (a) Crystalline Si nanostructure imaged at room temperature after STM fabrication (image courtesy of A. Ichimiya, Nagoya University). (b) Simplest continuum step model of the structure, neglecting the side facets[47] (image courtesy of D. Kandel, Weizmann Institute of Science).

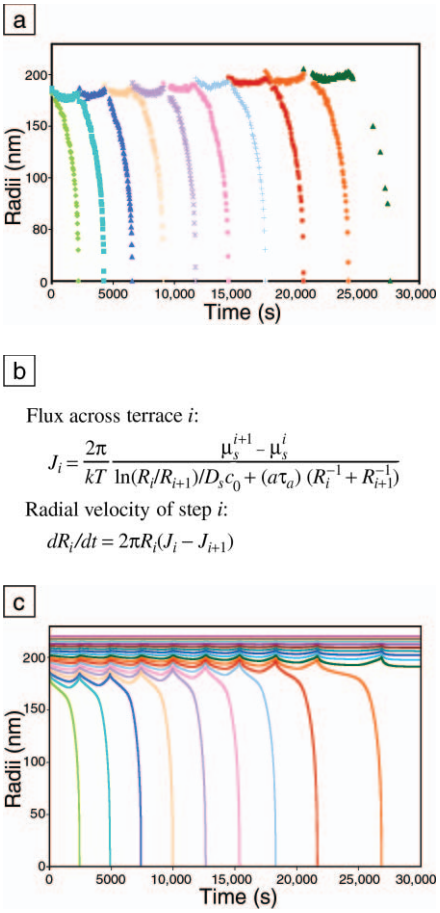

Figure 8. During the relaxation of a Pb crystallite following a rapid temperature decrease (see Figure 2), the circularly symmetric crystallite evolves via the sequential shrinking and disappearance of the top layers of atoms. (a) The experimentally measured radii of the shrinking layer and the second layer; a vertical line drawn through any two curves intersects the growing layer (upper curve of the pair) and the shrinking layer (bottom curve of the pair). The flux of atoms J between any two steps is governed by their difference in step chemical potential (see Figure 4) as well as the rates of atomic detachment from the step edge and diffusion across the terraces. Then, the rate of motion of each step is governed by the sum of the fluxes from its two neighboring steps, as shown in the coupled equations of motion in (b). (c) Numerical solution of the equations in (b) reproduces the experimental observations qualitatively well, with quantitative agreement hinging on careful attention to boundary conditions. (Numerical simulation by M. Degawa, University of Maryland.)

The mass transport can be modeled using the coupled equations of motion shown in Figure 8b, as well as reasonable estimates of the energetic parameters needed to evaluate the step chemical potentials.[21] The result of the simulation captures all of the qualitative features, and the time scale can be reproduced with reasonable choices for the kinetic parameters. The details of the evolution, particularly the slow-down in the rate of peeling as the final state is reached, depend on volume and the choice of the boundary conditions.[48]

As with the silicon pyramids, we can evaluate the strength of the driving force that causes the more than 500,000 atoms in each layer to pick up and move to the edges of the crystallite. In this case, the chemical potential gradients are even smaller than for the Si pyramids. Here, the ratio of the chemical potential to the thermal energy, μ/kT, is less than ~1%. However, even though the chemical potential gradients are tiny, compared with the thermal energy, there appears to be deterministic motion in the evolution of the structure. So, what does this mean in terms of the underlying fluctuations? Using our knowledge of the time constants with which atoms are moving on and off the step edge, we can find out that in fact there is a lot more uncertainty in this process than meets the eye. We find that each atom at the edge of the top shrinking layer is moving on and off the step edge an average of 1300 times before it decides to actually make the leap and diffuse across the terrace permanently to the edge of the crystallite. This impact of this stochastic behavior is most evident at the edges of the crystallite (see Figure 2c), where the step–step spacings are small.

First Passage and Persistence for Nanostructures

We would like to move forward from our classical, quasi-equilibrium picture of steps and the related thermodynamics describing nanostructures, and take the next step in understanding the potential impact of the stochastic nature of nanostructures. We can ask different types of questions to characterize this stochastic behavior. Instead of asking what the mean-squared displacement after a period of time t is, we can ask questions that might get at the stochastic nature of nanostructures by looking again at the fluctuations of individual steps. One relevant type of analysis is called the first-passage probability.[55] The generic first-passage question is, if a random walker starts out at position x at time zero, what is the *first* time that it might reach a position $x + \Delta x$? This question cannot be answered by taking correlation functions; it requires direct information on the position versus time itself. Of course, this is exactly what we can measure courtesy of a direct imaging technique like STM.

Experimentally, the first-passage probability is difficult to measure because it requires a lot of statistics. A related quantity is the persistence probability. This is essentially the integral of the first-passage probability, and we can get statistically significant tests of the persistence of step wandering with about the same measurement investment used for evaluating the correlation function.[56,57] The analysis is illustrated in Figure 9, which shows a schematic plot of the step position versus time. To do the analysis, we divide the total time of the measurement into equal bins (or intervals) of width Δt. Then, we define two classes of bins. A persistent bin is one where the path never gets back to the position at the beginning of the interval. In the figure, the path is persistent in the left-hand interval. In the right-hand interval, the path starts near the origin, and within the time interval Δt it crosses the original position again two times. So, the path is not persistent over this interval. By assessing the persistence over a large number of intervals, the persistence probability $p(\Delta t)$ for that time interval can be assessed. Then, the analysis is repeated for all other accessible values of Δt, giving the functional form of $p(t)$, the persistence probability as a function of time.

Theory predicts that the persistence probability will be a power law in time. For the case of wandering steps, the exponents have been predicted.[58] When step fluctuations are limited by attachment of atoms at the edges, as for the Al/Si system (Figure 6), the exponent is predicted to be 3/4. The persistence probability extracted from the Al/Si fluctuation data is shown in Figure 10. The power-law time scaling is clearly observed, with an exponent of 0.77 ± 0.03.[56] Interestingly, the magnitude of the persistence does not in fact depend on the temperature, even though the time constant governing the fluctuations ranges from 0.26 s at the lowest temperature to 1.2 ms at 970 K. Instead, the persistence curves depend only on the sampling time interval (the difference in time between repeated images of the same position on the step edge), as shown in Figure 10b.

The independence of the persistence magnitude is quite surprising, and it turns out to be a result of defining persistence in terms of the displacement *relative* to the start of each time interval.[59] There is another question we could ask:[56] at time interval Δt, what is the probability that the wandering step has reached a certain arbitrary position, perhaps one of physical significance such as the step average position, a defect, or an anti-step? This may represent a more interesting physical question than the relative displacement. In this case, the defined probability is called the survival probability, and it roughly decays exponentially with time, with a time constant related to the thermodynamic correlation time,[60] which is in turn related to the system size.

This example illustrates the beginning of the learning curve for relating physical step properties directly to their underlying stochastic behavior. Fifteen years ago, we were at this stage when we started looking at the equilibrium properties of steps. We wrestled with the ideas of how to get those equilibrium properties correlated with theory and how to turn the results into something useful in terms of predicting structural behavior. Here, we are hoping that addressing the stochastic aspects of the fluctuations of steps will allow us to make the same kind of progress, so that we can ultimately predict the stochastic properties of fluctuating nanoscale structures.

Conclusion

The evolution of solid structures via surface mass transport at the nano- to microscales occurs much more readily than

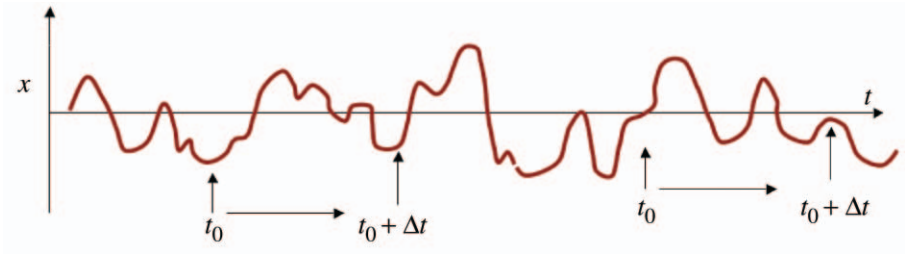

Figure 9. Given a path (e.g., the position of a single point on a step as a function of time), the persistence probability for a time Δt *is measured by evaluating the path throughout each time interval to see if the step returns to the starting point at the beginning of the interval. In the illustration shown, the path is persistent (i.e., does not return) in the left-hand interval and is not persistent (does return) in the right-hand interval.*

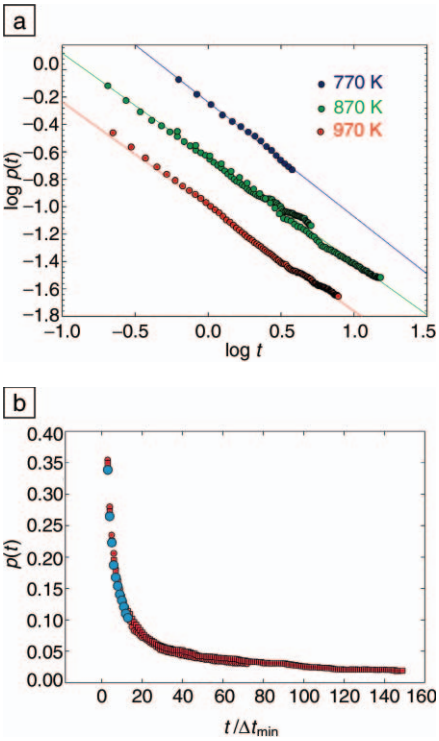

Figure 10. (a) Measured persistence probability for steps on Al/Si(111) for T = 970 K (red circles), T = 870 K (green circles), and T = 770 K (blue circles). log–log scale reveals power-law time dependence with an exponent of 0.77 ± 0.03. The data sets are spaced vertically for clarity. (b) Scaling the measurements in terms of the sampling time Δt_{min} interval causes a collapse of the persistence probability onto a single curve. Blue data points were measured with a sampling interval of 0.21 s, and the sampling interval for the red data points was 0.068 s. (Figures from D.B. Dougherty, University of Maryland.[57,58,60])

our intuition about solids might lead us to believe. We naturally think of solids as being resistant to shape change, but what we see experimentally is that it is relatively easy for large numbers of atoms—the kinds of numbers that are present in nanoscale structures—to pick up and move about on the surface cooperatively with substantial impact on nano- to microscale structures. We can predict quantitatively what goes on in such nanoscale mass transport by a simple and fundamental formalism. This formalism is based on defining *local* thermodynamic properties of the basic nanoscale building block, which is a step.

Among other things, the results show that extremely small driving forces (e.g., potential energy differences much less than *kT*) can cause large-scale and apparently deterministic structure changes. We can make these analyses and predictions because we can now do direct imaging with scanning tunneling microscopy (and other techniques) and map out the spatial and temporal distribution functions directly. Combined advances in experimental tools and theoretical understanding have brought us a long way toward quantifying the conceptual understanding of nanoscale mass transport that was established in the 1950s. As a result, we are now poised to explore one of the novel aspects of nanoscale science, which is life in a world where fluctuations represent a significant contribution to the overall properties of the structure. There are fascinating fundamental challenges in quantifying such stochastic behavior, with potential applications to issues such as switching between states, nucleation events, characterization of noise, and how our nanostructures might switch or change their properties abruptly in response to external fields.

Acknowledgments

The work reported here is a compilation of key points from many years of effort involving many collaborators, whose names can be found in the reference list. I am grateful to the National Science Foundation, Division of Materials Research, for long-standing support through the Presidential Young Investigator program, the Materials Research Group program, and most recently, the MRSEC program under grant DMR-00-80008. In addition, the Laboratory for Physical Science, College Park, has provided continuing stable and generous support, without which such long-term basic research would not be possible. Continuing support for this research is also being provided by the nanoscience initiatives of the NSF Nanoscience Interdisciplinary Research Team program and the Department of Energy.

References

1. C. Herring, *Phys. Rev.* **82** (1951) p. 87.
2. C. Herring, in *Structure and Properties of Crystal Surfaces*, edited by R. Gomer and C.S. Smith (University of Chicago Press, Chicago, 1953) p. 5.
3. J.W. Cahn, *J. de Phys.* **C6 (suppl.) 43** (1982) p. 199.
4. E.D. Williams and N.C. Bartelt, *Science* **251** (1991) p. 393.
5. E.D. Williams, R.J. Phaneuf, J. Wei, N.C. Bartelt, and T.L. Einstein, *Surf. Sci.* **294** (1993) p. 219.
6. W.W. Mullins, *Philos. Mag.* **6** (1961) p. 1313.
7. W.K. Burton, N. Cabrera, and F.C. Frank, *Phil. Trans. R. Soc. London* **243A** (1951) p. 299.
8. E.E. Gruber and W.W. Mullins, *J. Phys. Chem. Solids* **28** (1967) p. 875.
9. M.E. Fisher, *J. Stat. Phys.* **34** (1984) p. 667.
10. J. Villain, D.R. Grempel, and J. Lapujoulade, *J. Phys. F: Metal Phys.* **15** (1985) p. 809.
11. G. Ehrlich and K. Stolt, *Annu. Rev. Phys. Chem.* **31** (1980) p. 603.
12. B. Binnig and H. Rohrer, *Rev. Mod. Phys.* **59** (1987) p. 615.
13. E. Bauer, *Surf. Sci.* **299/300** (1994) p. 102.
14. N.C. Bartelt, R.M. Tromp, and E.D. Williams, *Phys. Rev. Lett.* **73** (1994) p. 1656.
15. K. Yagi, *Surf. Sci. Rep.* **17** (1993) p. 305.
16. N.C. Bartelt, J.L. Goldberg, T.L. Einstein, E.D. Williams, J.C. Heyraud, and J.J. Métois, *Phys. Rev. B* **48** (1993) p. 15453.
17. C. Rottman, M. Wortis, J.C. Heyraud, and J.J. Metois, *Phys. Rev. Lett.* **52** (1984) p. 1009.
18. A. Pavlovska, D. Dobrev, and E. Bauer, *Surf. Sci.* **326** (1995) p. 101.
19. A. Emundts, H.P. Bonzel, P. Wynblatt, K. Thürmer, J. Reutt-Robey, and E.D. Williams, *Surf. Sci.* **481** (2001) p. 13.
20. M. Nowicki, C. Bombis, A. Emundts and H.P. Bonzel, *Phys. Rev. B* **67** 075405 (2003).
21. K. Thürmer, J. Reutt-Robey, E.D. Williams, A. Emundts, H. Bonzel, and M. Uwaha, *Phys. Rev. Lett.* **87** 186102 (2001).
22. M. Uwaha and P. Nozières, in *Morphology and Growth Unit of Crystals*, edited by I. Sunagawa (Terra Scientific, Tokyo, 1989) p.17.
23. P. Nozieres, in *Solids Far from Equilibrium*, edited by C. Godrèche (Cambridge University Press, Cambridge, 1991) p. 1.
24. D.G. Vlachos, L.D. Schmidt, and R. Aris, *Phys. Rev. B* **47** (1993) p. 4896.
25. H. Yasunaga and A. Natori, *Surf. Sci. Rep.* **15** (1992) p. 205.
26. P.J. Rous, *Phys. Rev. B* **59** (1999) p. 7719.
27. D.-J. Liu and J.D. Weeks, *Phys. Rev. B* **57** (1998) p. 14891.
28. O. Pierre-Louis and T.L. Einstein, *Phys. Rev. B* **62** (2000) p. 13697.
29. P. Nozières, *J. de Phys.* **48** (1987) p. 1605.
30. N.C. Bartelt, T.L. Einstein, and E.D. Williams, *Surf. Sci.* **312** (1994) p. 411.
31. S.V. Khare and T.L. Einstein, *Phys. Rev. B* **57** (1998) p. 4782.
32. T. Ihle, C. Misbah, and O. Pierre-Louis, *Phys. Rev. B* **58** (1998) p. 2289.
33. H.-C. Jeong and J.D. Weeks, *Surf. Sci.* **432** (1999) p. 101.
34. H.-C. Jeong and E.D. Williams, *Surf. Sci. Rep.* **34** (1999) p. 171.
35. M. Giesen, *Prog. Surf. Sci.* **68** (2001) p. 1.
36. R.C. Nelson, T.L. Einstein, S.V. Khare, and P.J. Rous, *Surf. Sci.* **295** (1993) p. 462.
37. N.C. Bartelt, T.L. Einstein, and E.D. Williams, *Surf. Sci.* **276** (1992) p. 308.
38. N. Akutsu and Y. Akutsu, *J. Phys.: Condens. Matter* **11** (1999) p. 6635.
39. I. Lyubinetsky, D. Daugherty, H.L. Richards, T.L. Einstein, and E.D. Williams, *Surf. Sci.* **492** (2001) p. L671.
40. T. S. Rahman, A. Kara, and S. Durukanoglu, *J. Phys.: Condens. Matter* **15** (2003) p. S3197.
41. A. Karim, M. Rusanen, I.T. Koponen, T. Ala-Nissila, and T.S. Rahman, *Surf. Sci.* **554** (2004) p. L113.
42. C. Jayaprakash, C. Rottman, and W.F. Saam, *Phys. Rev. B* **30** (1984) p. 6549.
43. V.I. Marchenko and A.Y. Parshin, *Sov. Phys. JETP* **52** (1980) p. 129.

44. X.-S. Wang, J.L. Goldberg, N.C. Bartelt, T.L. Einstein, and E.D. Williams, *Phys. Rev. Lett.* **65** (1990) p. 2430.
45. H.L. Richards and T.L. Einstein, "Beyond the Wigner Distribution: Schrödinger Equations and Terrace Width Distributions," arXiv.org e-print archive, cond-mat/0008089 (accessed August 2004).
46. M. Uwaha, *J. Phys. Soc. Jpn.* **57** (1988) p. 1681.
47. N. Israeli and D. Kandel, *Phys. Rev. B* **60** (1999) p. 5946.
48. M. Degawa et al., in preparation.
49. M. Giesen, J. Frohn, M. Poensgen, J.F. Wolf, and H. Ibach, *J. Vac. Sci. Technol., A* **10** (1992) p. 2597.
50. L. Kuipers, M.S. Hoogeman, and J.W.M. Frenken, *Phys. Rev. Lett.* **71** (1993) p. 3517.
51. I. Lyubinetsky, D.B. Dougherty, T.L. Einstein, and E.D. Williams, *Phys. Rev. B* **66** 085327 (2002).
52. A. Ichimiya, Y. Tanaka, and K. Ishiyama, *Phys. Rev. Lett.* **76** (1996) p. 4721.
53. A. Ichimiya, K. Hayashi, E.D. Williams, T.L. Einstein, M. Uwaha, and K. Watanabe, *Phys. Rev. Lett.* **84** (2000) p. 3662.
54. A. Ichimiya, M. Suzuki, and S. Nishida, *Surf. Sci.* **493** (2001) p. 555.
55. S. Redner, *A Guide to First-Passage Processes* (Cambridge University Press, Cambridge, 2001).
56. D.B. Dougherty, I. Lyubinetsky, E.D. Williams, M. Constantin, C. Dasgupta, and S. Das Sarma, *Phys. Rev. Lett.* **89** 136102 (2002).
57. D.B. Dougherty, O. Bondarchuk, M. Degawa, and E.D. Williams, *Surf. Sci.* **527** (2002) p. L213.
58. J. Krug, H. Kallabis, S.N. Majumdar, S.J. Cornell, A.J. Bray, and C. Sire, *Phys. Rev.* **B56** (1997) p. 2702.
59. O. Bondarchuk, D.B. Dougherty, M. Degawa, E.D. Williams, M. Constantin, C. Dasgupta, and S. DasSarma, "Correlation Time for Step Structural Fluctuations," arXiv.org e-print archive, cond-mat/0408181 (accessed August 2004).
60. C. Dasgupta, M. Constantin, S. Das Sarma, and S.N. Majumdar, *Phys. Rev. E* **69** 022101 (2004). □

Ellen D. Williams, *Distinguished University Professor in the Department of Physics and the Institute for Physical Science and Technology at the University of Maryland, received her PhD degree in chemistry in 1981 from the California Institute of Technology. Immediately after obtaining her doctoral degree, she moved to the University of Maryland's Department of Physics and Astronomy as a postdoctoral research associate and later joined the faculty as an assistant professor.*

Her research has focused on experimental exploration of the statistical mechanics of solid surfaces and the consequences for nanoscale structures. Williams established the University of Maryland MRSEC (Materials Research Science and Engineering Center) in 1996 and continues to serve as director. She is active in communicating the excitement of science to nonscientists, and has given more than 50 talks in the last 15 years to pre-college, undergraduate, and nonacademic audiences. She was the director of the University of Maryland Chemical Physics program from 1993 to 1995.

Williams chaired the 1999 Materials Research Society Fall Meeting and the 2001 Gordon Conference on Thin Films and Crystal Growth. She has served on the executive committee of the Surface Science Division of the American Vacuum Society (1989–1990), the editorial advisory board of Surface Science *(1995–1998), the editorial boards for* Review of Scientific Instruments *(1991–1993) and* Nano Letters *(2001–present), and the board of reviewing editors for* Science *(2003–present), as well as on many panels and committees of professional societies. Her honors include being named a fellow of the American Academy of Arts and Sciences (2003) and receiving the American Physical Society's David Adler Lectureship (2001).*

Williams can be reached by e-mail at edw@physics.umd.edu.